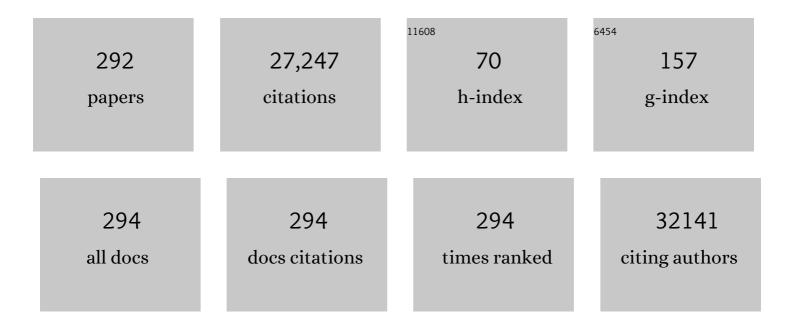
## Li-Jie Ci

## List of Publications by Year in descending order

Source: https://exaly.com/author-pdf/3237755/publications.pdf Version: 2024-02-01



Ludie Cu

#	Article	IF	CITATIONS
1	A novel coral-like garnet for high-performance PEO-based all solid-state batteries. Science China Materials, 2022, 65, 364-372.	3.5	20
2	One-step synthesis of hollow urchin-like Ag2Mn8O16 for long-life Li-O2 battery. Journal of Alloys and Compounds, 2022, 892, 162137.	2.8	4
3	Alleviation role of functional carbon nanodots for tomato growth and soil environment under drought stress. Journal of Hazardous Materials, 2022, 423, 127260.	6.5	14
4	Sheet-like garnet structure design for upgrading PEO-based electrolyte. Chemical Engineering Journal, 2022, 429, 132343.	6.6	42
5	In situ construction of a flexible interlayer for durable solid-state lithium metal batteries. Carbon, 2022, 187, 13-21.	5.4	13
6	Carbon Nanotubesâ€Based Electrocatalysts: Structural Regulation, Support Effect, and Synchrotronâ€Based Characterization. Advanced Functional Materials, 2022, 32, 2106684.	7.8	14
7	In situ modified sulfide solid electrolyte enabling stable lithium metal batteries. Journal of Power Sources, 2022, 518, 230739.	4.0	25
8	Reversible LiOH chemistry in Li-O2 batteries with free-standing Ag/δ-MnO2 nanoflower cathode. Science China Materials, 2022, 65, 1431-1442.	3.5	9
9	Li <sub>2</sub> CO <sub>3</sub> : Insights into Its Blocking Effect on Li-Ion Transfer in Garnet Composite Electrolytes. ACS Applied Energy Materials, 2022, 5, 2853-2861.	2.5	17
10	Focusing on the Subsequent Coulombic Efficiencies of SiO <sub><i>x</i></sub> : Initial High-Temperature Charge after Over-Capacity Prelithiation for High-Efficiency SiO <sub><i>x</i></sub> -Based Full-Cell Battery. ACS Applied Materials & Interfaces, 2022, 14, 14284-14292.	4.0	22
11	Enhanced ions and electrons transmission enables high-performance KxMnO@C cathode for hybrid supercapacitors. Ceramics International, 2022, 48, 16516-16521.	2.3	2
12	Commercial carbon cloth: An emerging substrate for practical lithium metal batteries. Energy Storage Materials, 2022, 48, 172-190.	9.5	50
13	Functional carbon nanodots improve soil quality and tomato tolerance in saline-alkali soils. Science of the Total Environment, 2022, 830, 154817.	3.9	17
14	VS4 nanoarrays pillared Ti3C2Tx with enlarged interlayer spacing as anode for advanced lithium/sodium ion battery and hybrid capacitor. Journal of Power Sources, 2022, 534, 231412.	4.0	26
15	Trash to treasure: recycling discarded agarose gel for practical Na/K-ion batteries. Journal of Materials Chemistry A, 2022, 10, 15026-15035.	5.2	7
16	Interlayer Engineering of K <sub><i>x</i></sub> MnO <sub>2</sub> Enables Superior Alkali Metal Ion Storage for Advanced Hybrid Capacitors. ChemElectroChem, 2022, 9, .	1.7	9
17	Low-cost and facile synthesis of LAGP solid state electrolyte via a co-precipitation method. Applied Physics Letters, 2022, 121, 023904.	1.5	8
18	Indium doped sulfide solid electrolyte with tamed lithium dendrite and improved ionic conductivity for all-solid-state battery applications. Journal of Power Sources, 2022, 542, 231794.	4.0	9

#	Article	IF	CITATIONS
19	Carbon aerogel reinforced PDMS nanocomposites with controllable and hierarchical microstructures for multifunctional wearable devices. Carbon, 2021, 171, 758-767.	5.4	29
20	Ag+ preintercalation enabling high performance AgxMnO2 cathode for aqueous Li-ion and Na-ion hybrid supercapacitors. Journal of Power Sources, 2021, 484, 229316.	4.0	8
21	Foldable potassium-ion batteries enabled by free-standing and flexible SnS <sub>2</sub> @C nanofibers. Energy and Environmental Science, 2021, 14, 424-436.	15.6	142
22	Preparation and characterization of Sn-doped In2.77S4 nanosheets as a visible-light-induced photocatalyst for tetracycline degradation. Journal of Materials Science: Materials in Electronics, 2021, 32, 2822-2831.	1.1	8
23	Fast and stable K-ion storage enabled by synergistic interlayer and pore-structure engineering. Nano Research, 2021, 14, 4502-4511.	5.8	36
24	Spontaneous In Situ Surface Alloying of Li-Zn Derived from a Novel Zn2+-Containing Solid Polymer Electrolyte for Steady Cycling of Li Metal Battery. ACS Sustainable Chemistry and Engineering, 2021, 9, 4282-4292.	3.2	4
25	Bifunctional In Situ Polymerized Interface for Stable LAGPâ€Based Lithium Metal Batteries. Advanced Materials Interfaces, 2021, 8, 2100072.	1.9	22
26	Lewis Acidity Organoboronâ€Modified Liâ€Rich Cathode Materials for Highâ€Performance Lithiumâ€lon Batteries. Advanced Materials Interfaces, 2021, 8, 2002113.	1.9	11
27	A graphene oxide coated sulfide-based solid electrolyte for dendrite-free lithium metal batteries. Carbon, 2021, 177, 52-59.	5.4	24
28	Phosphorous-doped bimetallic sulfides embedded in heteroatom-doped carbon nanoarrays for flexible all-solid-state supercapacitors. Science China Materials, 2021, 64, 2439-2453.	3.5	19
29	Enhanced Air and Electrochemical Stability of Li <sub>7</sub> P <sub>3</sub> S <sub>11</sub> –Based Solid Electrolytes Enabled by Aliovalent Substitution of SnO <sub>2</sub> . Advanced Materials Interfaces, 2021, 8, 2100368.	1.9	24
30	Rational construction of ternary ZnNiP arrayed structures derived from 2D MOFs for advanced hybrid supercapacitors and Zn batteries. Electrochimica Acta, 2021, 387, 138548.	2.6	25
31	Mechanistic Insights into the Structural Modulation of Transition Metal Selenides to Boost Potassium Ion Storage Stability. ACS Nano, 2021, 15, 14697-14708.	7.3	44
32	Potassium Ions Regulated the Disproportionation of Silicon Monoxide Boosting Its Performance for Lithium-Ion Battery Anodes. Energy & Fuels, 2021, 35, 16202-16211.	2.5	8
33	Ag <sub><i>x</i></sub> Mn <sub>8</sub> O <sub>16</sub> Cathode Enables High-Performance Aqueous Li-Ion Hybrid Supercapacitors. Energy & Fuels, 2021, 35, 15101-15107.	2.5	3
34	Guest ions pre-intercalation strategy of manganese-oxides for supercapacitor and battery applications. Journal of Energy Chemistry, 2021, 60, 480-493.	7.1	36
35	A high-energy, long cycle life aqueous hybrid supercapacitor enabled by efficient battery electrode and widened potential window. Journal of Alloys and Compounds, 2021, 877, 160273.	2.8	8
36	Three-dimensional hollow nitrogen-doped carbon shells enclosed monodisperse CoP nanoparticles for long cycle-life sodium storage. Electrochimica Acta, 2021, 395, 139112.	2.6	19

#	Article	IF	CITATIONS
37	Effects of functional carbon nanodots on water hyacinth response to Cd/Pb stress: Implication for phytoremediation. Journal of Environmental Management, 2021, 299, 113624.	3.8	15
38	Accelerating the activation of Li <sub>2</sub> MnO <sub>3</sub> in Li-rich high-Mn cathodes to improve its electrochemical performance. Nanoscale, 2021, 13, 4921-4930.	2.8	17
39	ZnCl <sub>2</sub> -activated carbon from soybean dregs as a high efficiency adsorbent for cationic dye removal: isotherm, kinetic, and thermodynamic studies. Environmental Technology (United) Tj ETQq1 1 (	0.7843 <b>1.≇</b> rgB	T / <b>Q</b> #erlock 1
40	Composite solid electrolyte of Na3PS4-PEO for all-solid-state SnS2/Na batteries with excellent interfacial compatibility between electrolyte and Na metal. Journal of Energy Chemistry, 2020, 41, 73-78.	7.1	48
41	Boron-doped graphene coated Au@SnO2 for high-performance triethylamine gas detection. Materials Chemistry and Physics, 2020, 239, 121961.	2.0	21
42	Potassium pre-inserted K1.04Mn8O16 as cathode materials for aqueous Li-ion and Na-ion hybrid capacitors. Journal of Energy Chemistry, 2020, 46, 53-61.	7.1	40
43	Nitrogen and sulfur co-doped porous carbon fibers film for flexible symmetric all-solid-state supercapacitors. Carbon, 2020, 158, 456-464.	5.4	72
44	Enhanced plant antioxidant capacity and biodegradation of phenol by immobilizing peroxidase on amphoteric nitrogen-doped carbon dots. Catalysis Communications, 2020, 134, 105847.	1.6	22
45	Enhanced bioaccumulation efficiency and tolerance for Cd (â¡) in Arabidopsis thaliana by amphoteric nitrogen-doped carbon dots. Ecotoxicology and Environmental Safety, 2020, 190, 110108.	2.9	21
46	Facile construction of a hybrid artificial protective layer for stable lithium metal anode. Chemical Engineering Journal, 2020, 391, 123542.	6.6	25
47	Lightweight graphene oxide-based sponges with high compressibility and durability for dye adsorption. Carbon, 2020, 160, 54-63.	5.4	30
48	Stable Lithium Anode of Li–O <sub>2</sub> Batteries in a Wet Electrolyte Enabled by a High-Current Treatment. Journal of Physical Chemistry Letters, 2020, 11, 172-178.	2.1	16
49	Stable lithium metal anode enabled by an artificial multi-phase composite protective film. Journal of Power Sources, 2020, 448, 227547.	4.0	30
50	Cold-pressing PEO/LAGP composite electrolyte for integrated all-solid-state lithium metal battery. Solid State Ionics, 2020, 345, 115156.	1.3	40
51	Structural Engineering of SnS <sub>2</sub> Encapsulated in Carbon Nanoboxes for Highâ€Performance Sodium/Potassiumâ€ion Batteries Anodes. Small, 2020, 16, e2005023.	5.2	120
52	High performance hierarchically nanostructured graphene oxide/covalent organic framework hybrid membranes for stable organic solvent nanofiltration. Applied Materials Today, 2020, 20, 100791.	2.3	23
53	Impacts of surface chemistry of functional carbon nanodots on the plant growth. Ecotoxicology and Environmental Safety, 2020, 206, 111220.	2.9	22
54	Ultrathin carbon nanosheets for highly efficient capacitive K-ion and Zn-ion storage. Journal of Materials Chemistry A, 2020, 8, 22874-22885.	5.2	58

#	Article	IF	CITATIONS
55	Flexible rGO @ Nonwoven Fabrics' Membranes Guide Stable Lithium Metal Anodes for Lithium–Oxygen Batteries. ACS Applied Energy Materials, 2020, 3, 7944-7951.	2.5	9
56	SnO <sub>2</sub> microrods based triethylamine gas sensor. IOP Conference Series: Materials Science and Engineering, 2020, 772, 012058.	0.3	5
57	Ballâ€Milling Strategy for Fast and Stable Potassiumâ€Ion Storage in Antimonyâ€ <i>Carbon</i> Composite Anodes. ChemElectroChem, 2020, 7, 4587-4593.	1.7	6
58	Study on Ag2WO4/g-C3N4 Nanotubes as an Efficient Photocatalyst for Degradation of Rhodamine B. Journal of Inorganic and Organometallic Polymers and Materials, 2020, 30, 4847-4857.	1.9	17
59	Microwave assisted crystalline and morphology evolution of flower-like Fe2O3@ iron doped K-birnessite composite and its application for lithium ion storage. Applied Surface Science, 2020, 525, 146513.	3.1	18
60	Enhanced Electrochemical Performance of Li <sub>1.2</sub> [Mn <sub>0.54</sub> Co <sub>0.13</sub> Ni <sub>0.13</sub> ]O <sub>2</sub> Enabled by Synergistic Effect of Li <sub>1.5</sub> Na <sub>0.5</sub> SiO <sub>3</sub> Modification. Advanced Materials Interfaces, 2020, 7, 2000378.	1.9	9
61	Facilely tunable core-shell Si@SiOx nanostructures prepared in aqueous solution for lithium ion battery anode. Electrochimica Acta, 2020, 342, 136068.	2.6	52
62	Lithium-conducting covalent-organic-frameworks as artificial solid-electrolyte-interphase on silicon anode for high performance lithium ion batteries. Nano Energy, 2020, 72, 104657.	8.2	93
63	Ag doped urchin-like α-MnO2 toward efficient and bifunctional electrocatalysts for Li-O2 batteries. Nano Research, 2020, 13, 2356-2364.	5.8	27
64	Bio-inspired multiple-stimuli responsive porous materials with switchable flexibility and programmable shape morphing capability. Carbon, 2020, 161, 702-711.	5.4	12
65	Promotion effect of nitrogen-doped functional carbon nanodots on the early growth stage of plants. Oxford Open Materials Science, 2020, 1, .	0.5	5
66	High Current Enabled Stable Lithium Anode for Ultralong Cycling Life of Lithium–Oxygen Batteries. ACS Applied Materials & Interfaces, 2019, 11, 30793-30800.	4.0	21
67	Mesoporous Mn2O3 rods as a highly efficient catalyst for Li-O2 battery. Journal of Power Sources, 2019, 435, 226833.	4.0	29
68	Artificial Solid Electrolyte Interphase Coating to Reduce Lithium Trapping in Silicon Anode for High Performance Lithiumâ€ion Batteries. Advanced Materials Interfaces, 2019, 6, 1901187.	1.9	54
69	Reduced graphene oxide/SnO2@Au heterostructure for enhanced ammonia gas sensing. Chemical Physics Letters, 2019, 737, 136829.	1.2	19
70	Li metal-free rechargeable all-solid-state Li2S/Si battery based on Li7P3S11 electrolyte. Journal of Solid State Electrochemistry, 2019, 23, 3145-3151.	1.2	23
71	Nitrogen-doped carbon derived from pre-oxidized pitch for surface dominated potassium-ion storage. Carbon, 2019, 155, 601-610.	5.4	110
72	Selective Chemical Enhancement via Graphene Oxide in Infrared Attenuated Total Reflection Spectroscopy. Journal of Physical Chemistry C, 2019, 123, 25286-25293.	1.5	5

#	Article	IF	CITATIONS
73	Boron nitride doped Li7P3S11 solid electrolyte with improved interfacial compatibility and application in all-solid-state Li/S battery. Journal of Materials Science: Materials in Electronics, 2019, 30, 19119-19125.	1.1	20
74	Well-defined cobalt sulfide nanoparticles locked in 3D hollow nitrogen-doped carbon shells for superior lithium and sodium storage. Energy Storage Materials, 2019, 18, 114-124.	9.5	62
75	A Review of the Role of Solvents in Formation of High-Quality Solution-Processed Perovskite Films. ACS Applied Materials & Interfaces, 2019, 11, 7639-7654.	4.0	113
76	Self-supported multidimensional Ni–Fe phosphide networks with holey nanosheets for high-performance all-solid-state supercapacitors. Journal of Materials Chemistry A, 2019, 7, 17386-17399.	5.2	72
77	Monometallic nanoporous nickel with high catalytic performance towards hydrazine electro-conversion and its DFT calculations. Electrochimica Acta, 2019, 317, 449-458.	2.6	8
78	Integrated nanocomposite of LiMn2O4/graphene/carbon nanotubes with pseudocapacitive properties as superior cathode for aqueous hybrid capacitors. Journal of Electroanalytical Chemistry, 2019, 842, 74-81.	1.9	38
79	Effective synthetic strategy for Zn <sub>0.76</sub> Co <sub>0.24</sub> S encapsulated in stabilized N-doped carbon nanoarchitecture towards ultra-long-life hybrid supercapacitors. Journal of Materials Chemistry A, 2019, 7, 14670-14680.	5.2	59
80	Surfaceâ€Confined SnS <sub>2</sub> @C@rGO as Highâ€Performance Anode Materials for Sodium―and Potassiumâ€Ion Batteries. ChemSusChem, 2019, 12, 2689-2700.	3.6	98
81	Hierarchically porous carbon supported Sn4P3 as a superior anode material for potassium-ion batteries. Energy Storage Materials, 2019, 23, 367-374.	9.5	120
82	Non-Flammable Phosphate Electrolyte with High Salt-to-Solvent Ratios for Safe Potassium-Ion Battery. Journal of the Electrochemical Society, 2019, 166, A1217-A1222.	1.3	48
83	High efficient adsorption and storage of iodine on S, N co-doped graphene aerogel. Journal of Hazardous Materials, 2019, 373, 705-715.	6.5	73
84	Growth direction control of lithium dendrites in a heterogeneous lithiophilic host for ultra-safe lithium metal batteries. Journal of Power Sources, 2019, 416, 141-147.	4.0	31
85	Tunable synthesis of LixMnO2 nanowires for aqueous Li-ion hybrid supercapacitor with high rate capability and ultra-long cycle life. Journal of Power Sources, 2019, 413, 302-309.	4.0	63
86	Fabrication of Perovskite Films with Long Carrier Lifetime for Efficient Perovskite Solar Cells from Low-Toxicity 1-Ethyl-2-Pyrrolidone. ACS Applied Energy Materials, 2019, 2, 320-327.	2.5	4
87	Surface-enhanced infrared attenuated total reflection spectroscopy via carbon nanodots for small molecules in aqueous solution. Analytical and Bioanalytical Chemistry, 2019, 411, 1863-1871.	1.9	10
88	Investigation on Crystallization of CH <sub>3</sub> NH <sub>3</sub> PbI <sub>3</sub> Perovskite and Its Intermediate Phase from Polar Aprotic Solvents. Crystal Growth and Design, 2019, 19, 959-965.	1.4	22
89	NaCa2Si3O8(OH)/PEDOT:PSS composite nanowires as anode materials for lithium-ion batteries. Chemical Physics Letters, 2019, 715, 40-44.	1.2	4
90	Potassium gluconate-derived N/S Co-doped carbon nanosheets as superior electrode materials for supercapacitors and sodium-ion batteries. Journal of Power Sources, 2019, 414, 308-316.	4.0	87

#	Article	IF	CITATIONS
91	Dissolution and recrystallization of perovskite induced by N-methyl-2-pyrrolidone in a closed steam annealing method. Journal of Energy Chemistry, 2019, 30, 78-83.	7.1	16
92	Nanocarbon Composites for Energy Storage Applications. ECS Meeting Abstracts, 2019, , .	0.0	0
93	Enhanced efficiency of perovskite solar cells by introducing controlled chloride incorporation into MAPbI3 perovskite films. Electrochimica Acta, 2018, 275, 1-7.	2.6	25
94	Crystallization of CH <sub>3</sub> NH <sub>3</sub> PbI <sub>3â^'x</sub> Br <sub>x</sub> perovskite from micro-droplets of lead acetate precursor solution. CrystEngComm, 2018, 20, 3058-3065.	1.3	5
95	Green, Scalable, and Controllable Fabrication of Nanoporous Silicon from Commercial Alloy Precursors for High-Energy Lithium-Ion Batteries. ACS Nano, 2018, 12, 4993-5002.	7.3	269
96	High annealing temperature induced rapid grain coarsening for efficient perovskite solar cells. Journal of Colloid and Interface Science, 2018, 524, 483-489.	5.0	35
97	Graphene oxide based membrane intercalated by nanoparticles for high performance nanofiltration application. Chemical Engineering Journal, 2018, 347, 12-18.	6.6	143
98	High performance graphene oxide nanofiltration membrane prepared by electrospraying for wastewater purification. Carbon, 2018, 130, 487-494.	5.4	144
99	Fabrication of Perovskite Films with Large Columnar Grains via Solvent-Mediated Ostwald Ripening for Efficient Inverted Perovskite Solar Cells. ACS Applied Energy Materials, 2018, 1, 868-875.	2.5	58
100	Commercial expanded graphite as a low–cost, long-cycling life anode for potassium–ion batteries with conventional carbonate electrolyte. Journal of Power Sources, 2018, 378, 66-72.	4.0	299
101	Nanostructured LiMn2O4 composite as high-rate cathode for high performance aqueous Li-ion hybrid supercapacitors. Journal of Power Sources, 2018, 392, 116-122.	4.0	46
102	Li7P3S11 solid electrolyte coating silicon for high-performance lithium-ion batteries. Electrochimica Acta, 2018, 276, 325-332.	2.6	18
103	Experimental investigation of mechanical properties of UV-Curable 3D printing materials. Polymer, 2018, 145, 88-94.	1.8	45
104	A large-area free-standing graphene oxide multilayer membrane with high stability for nanofiltration applications. Chemical Engineering Journal, 2018, 345, 536-544.	6.6	136
105	Aluminum/graphene composites with enhanced heat-dissipation properties by in-situ reduction of graphene oxide on aluminum particles. Journal of Alloys and Compounds, 2018, 748, 854-860.	2.8	103
106	Three-dimensional iron sulfide-carbon interlocked graphene composites for high-performance sodium-ion storage. Nanoscale, 2018, 10, 7851-7859.	2.8	56
107	Dendrite-free Li metal anode enabled by a 3D free-standing lithiophilic nitrogen-enriched carbon sponge. Journal of Power Sources, 2018, 386, 77-84.	4.0	65
108	Vacuum distillation derived 3D porous current collector for stable lithium–metal batteries. Nano Energy, 2018, 47, 503-511.	8.2	221

#	Article	IF	CITATIONS
109	Synergic mechanism of adsorption and metal-free catalysis for phenol degradation by N-doped graphene aerogel. Chemosphere, 2018, 191, 389-399.	4.2	54
110	Flexible all-solid-state supercapacitors based on freestanding, binder-free carbon nanofibers@polypyrrole@graphene film. Chemical Engineering Journal, 2018, 334, 184-190.	6.6	113
111	Two-step fabrication of nanoporous copper films with tunable morphology for SERS application. Applied Surface Science, 2018, 427, 1271-1279.	3.1	30
112	High-performance red phosphorus/carbon nanofibers/graphene free-standing paper anode for sodium ion batteries. Journal of Materials Chemistry A, 2018, 6, 1574-1581.	5.2	65
113	Surfactant-dependent flower- and grass-like Zn <sub>0.76</sub> Co <sub>0.24</sub> S/Co <sub>3</sub> S <sub>4</sub> for high-performance all-solid-state asymmetric supercapacitors. Journal of Materials Chemistry A, 2018, 6, 22830-22839.	5.2	60
114	Micron-Sized Nanoporous Antimony with Tunable Porosity for High-Performance Potassium-Ion Batteries. ACS Nano, 2018, 12, 12932-12940.	7.3	223
115	Enhanced Cycling Performance of Li–O <sub>2</sub> Battery by Using a Li <sub>3</sub> PO <sub>4</sub> -Protected Lithium Anode in DMSO-Based Electrolyte. ACS Applied Energy Materials, 2018, 1, 5511-5517.	2.5	20
116	Reduced graphene oxide wrapped Au@ZnO core-shell structure for highly selective triethylamine gas sensing application at a low temperature. Sensors and Actuators A: Physical, 2018, 283, 128-133.	2.0	34
117	Hierarchical layer-by-layer porous FeCo <sub>2</sub> S <sub>4</sub> @Ni(OH) <sub>2</sub> arrays for all-solid-state asymmetric supercapacitors. Journal of Materials Chemistry A, 2018, 6, 20480-20490.	5.2	102
118	Investigation of the gas-sensitive properties for methanol detection based on ZnO/SnO2 heterostructure. IOP Conference Series: Materials Science and Engineering, 2018, 392, 032016.	0.3	2
119	Facile Fabrication of Nitrogenâ€Doped Porous Carbon as Superior Anode Material for Potassiumâ€lon Batteries. Advanced Energy Materials, 2018, 8, 1802386.	10.2	393
120	In Situ Synthesis of a Lithiophilic Ag-Nanoparticles-Decorated 3D Porous Carbon Framework toward Dendrite-Free Lithium Metal Anodes. ACS Sustainable Chemistry and Engineering, 2018, 6, 15219-15227.	3.2	43
121	Reduced graphene oxide decorated Pt activated SnO2 nanoparticles for enhancing methanol sensing performance. Journal of Alloys and Compounds, 2018, 762, 8-15.	2.8	39
122	Lithium Dendrite Suppression and Enhanced Interfacial Compatibility Enabled by an Ex Situ SEI on Li Anode for LAGP-Based All-Solid-State Batteries. ACS Applied Materials & Interfaces, 2018, 10, 18610-18618.	4.0	123
123	Improved interfacial floatability of superhydrophobic and compressive S, N co-doped graphene aerogel by electrostatic spraying for highly efficient organic pollutants recovery from water. Applied Surface Science, 2018, 457, 780-788.	3.1	22
124	Synergistic double-shell coating of graphene and Li4SiO4 on silicon for high performance lithium-ion battery application. Diamond and Related Materials, 2018, 88, 60-66.	1.8	11
125	High-damping and conducting epoxy nanocomposite using both zinc oxide particles and carbon nanofibers. Journal of Materiomics, 2018, 4, 187-193.	2.8	3
126	Hollow nanoporous red phosphorus as an advanced anode for sodium-ion batteries. Journal of Materials Chemistry A, 2018, 6, 12992-12998.	5.2	36

#	Article	IF	CITATIONS
127	Stable all-solid-state potassium battery operating at room temperature with a composite polymer electrolyte and a sustainable organic cathode. Journal of Power Sources, 2018, 399, 294-298.	4.0	109
128	Green and facile synthesis of nanosized polythiophene as an organic anode for high-performance potassium-ion battery. Functional Materials Letters, 2018, 11, 1840003.	0.7	20
129	Fabrication and electromagnetic properties of carbon-based iron nitride composite. Journal of Magnetism and Magnetic Materials, 2018, 466, 22-27.	1.0	29
130	Enhanced heterogeneous activation of peroxydisulfate by S, N co-doped graphene via controlling S, N functionalization for the catalytic decolorization of dyes in water. Chemosphere, 2018, 210, 120-128.	4.2	25
131	Self-supporting soft carbon fibers as binder-free and flexible anodes for high-performance sodium-ion batteries. Materials Technology, 2018, 33, 810-814.	1.5	12
132	Li7P3S11/poly(ethylene oxide) hybrid solid electrolytes with excellent interfacial compatibility for all-solid-state batteries. Journal of Power Sources, 2018, 400, 212-217.	4.0	88
133	Sandwichâ€Like FeCl <sub>3</sub> @C as Highâ€Performance Anode Materials for Potassiumâ€Ion Batteries. Advanced Materials Interfaces, 2018, 5, 1800606.	1.9	53
134	Core-shell structured carbon nanofibers yarn@polypyrrole@graphene for high performance all-solid-state fiber supercapacitors. Carbon, 2018, 138, 264-270.	5.4	110
135	Facile preparation of fullerene nanorods for high-performance lithium-sulfur batteries. Materials Letters, 2018, 228, 175-178.	1.3	13
136	Nanoporous Red Phosphorus on Reduced Graphene Oxide as Superior Anode for Sodium-Ion Batteries. ACS Nano, 2018, 12, 7380-7387.	7.3	120
137	Metal–Organic Framework Derived Iron Sulfide–Carbon Core–Shell Nanorods as a Conversion-Type Battery Material. ACS Sustainable Chemistry and Engineering, 2017, 5, 5039-5048.	3.2	82
138	Control of the morphology of PbI <sub>2</sub> films for efficient perovskite solar cells by strong Lewis base additives. Journal of Materials Chemistry C, 2017, 5, 7458-7464.	2.7	57
139	Fabrication of high quality perovskite films by modulating the Pb–O bonds in Lewis acid–base adducts. Journal of Materials Chemistry A, 2017, 5, 8416-8422.	5.2	73
140	Graphene encapsulated Fe <sub>3</sub> O <sub>4</sub> nanorods assembled into a mesoporous hybrid composite used as a high-performance lithium-ion battery anode material. Materials Chemistry Frontiers, 2017, 1, 1185-1193.	3.2	41
141	Enhanced performance of perovskite solar cells by strengthening a self-embedded solvent annealing effect in perovskite precursor films. RSC Advances, 2017, 7, 49144-49150.	1.7	11
142	Elucidating the Key Role of a Lewis Base Solvent in the Formation of Perovskite Films Fabricated from the Lewis Adduct Approach. ACS Applied Materials & Interfaces, 2017, 9, 32868-32875.	4.0	47
143	Tensile properties of millimeter-long multi-walled carbon nanotubes. Scientific Reports, 2017, 7, 9512.	1.6	66
144	A heart-coronary arteries structure of carbon nanofibers/graphene/silicon composite anode for high performance lithium ion batteries. Scientific Reports, 2017, 7, 9642.	1.6	28

#	Article	IF	CITATIONS
145	Lithium metal protection enabled by in-situ olefin polymerization for high-performance secondary lithium sulfur batteries. Journal of Power Sources, 2017, 363, 193-198.	4.0	43
146	Walnut-inspired microsized porous silicon/graphene core–shell composites for high-performance lithium-ion battery anodes. Nano Research, 2017, 10, 4274-4283.	5.8	72
147	A titanium-based metal–organic framework as an ultralong cycle-life anode for PIBs. Chemical Communications, 2017, 53, 8360-8363.	2.2	94
148	High performance agar/graphene oxide composite aerogel for methylene blue removal. Carbohydrate Polymers, 2017, 155, 345-353.	5.1	251
149	Hierarchical Porous Chitosan Sponges as Robust and Recyclable Adsorbents for Anionic Dye Adsorption. Scientific Reports, 2017, 7, 18054.	1.6	94
150	Perovskite Solar Cells Fabricated by Using an Environmental Friendly Aprotic Polar Additive of 1,3-Dimethyl-2-imidazolidinone. Nanoscale Research Letters, 2017, 12, 632.	3.1	19
151	A novel Lithium/Sodium hybrid aqueous electrolyte for hybrid supercapacitors based on LiFePO <sub>4</sub> and activated carbon. Functional Materials Letters, 2016, 09, 1642008.	0.7	15
152	Enhancing the safety and electrochemical performance of ether based lithium sulfur batteries by introducing an efficient flame retarding additive. RSC Advances, 2016, 6, 53560-53565.	1.7	19
153	Metal–organic framework-derived graphene@nitrogen doped carbon@ultrafine TiO <sub>2</sub> nanocomposites as high rate and long-life anodes for sodium ion batteries. Chemical Communications, 2016, 52, 12810-12812.	2.2	48
154	Unveil the Sizeâ€Đependent Mechanical Behaviors of Individual CNT/SiC Composite Nanofibers by In Situ Tensile Tests in SEM. Small, 2016, 12, 4486-4491.	5.2	20
155	Mental-organic framework derived CuO hollow spheres as high performance anodes for sodium ion battery. Materials Technology, 2016, 31, 497-500.	1.5	17
156	MnO <sub>2</sub> nanotubes with a water soluble binder as high performance sodium storage materials. RSC Advances, 2016, 6, 103579-103584.	1.7	18
157	Carbon coated copper sulfides nanosheets synthesized via directly sulfurizing Metal-Organic Frameworks for lithium batteries. Materials Letters, 2016, 181, 340-344.	1.3	29
158	Facile hydrothermal growth of VO2 nanowire, nanorod and nanosheet arrays as binder free cathode materials for sodium batteries. RSC Advances, 2016, 6, 14314-14320.	1.7	13
159	Towards methyl orange degradation by direct sunlight using coupled TiO2 nanoparticles and carbonized cotton T-shirt. Applied Materials Today, 2016, 3, 57-62.	2.3	12
160	A novel bifunctional additive for 5 V-class, high-voltage lithium ion batteries. RSC Advances, 2016, 6, 7224-7228.	1.7	23
161	Hierarchical reinforcement of randomly-oriented carbon nanotube mats by ion irradiation. Carbon, 2016, 99, 491-501.	5.4	7
162	Biphenyl as overcharge protection additive for nonaqueous sodium batteries. RSC Advances, 2015, 5, 96649-96652.	1.7	20

#	Article	IF	CITATIONS
163	Nonflammable electrolyte for safer non-aqueous sodium batteries. Journal of Materials Chemistry A, 2015, 3, 14539-14544.	5.2	64
164	Chemical dealloying synthesis of porous silicon anchored by in situ generated graphene sheets as anode material for lithium-ion batteries. Journal of Power Sources, 2015, 287, 177-183.	4.0	102
165	Nanotubes within transition metal silicate hollow spheres: Facile preparation and superior lithium storage performances. Materials Research Bulletin, 2015, 70, 573-578.	2.7	27
166	One-pot solvothermal synthesis of graphene wrapped rice-like ferrous carbonate nanoparticles as anode materials for high energy lithium-ion batteries. Nanoscale, 2015, 7, 232-239.	2.8	46
167	One-step, room temperature, colorimetric melamine sensing using an in-situ formation of silver nanoparticles through modified Tollens process. Spectrochimica Acta - Part A: Molecular and Biomolecular Spectroscopy, 2015, 137, 281-285.	2.0	25
168	Low temperature synthesis of lead germanate (PbGeO3)/polypyrrole (PPy) nanocomposites and their lithium storage performance. Materials Research Bulletin, 2014, 57, 238-242.	2.7	10
169	Direct growth of aligned graphitic nanoribbons from a DNA template by chemical vapour deposition. Nature Communications, 2013, 4, 2402.	5.8	47
170	Cu3V2O8 hollow spheres in photocatalysis and primary lithium batteries. Solid State Sciences, 2013, 25, 15-21.	1.5	42
171	Tuning the Dirac Point in CVD-Grown Graphene through Solution Processed n-Type Doping with 2-(2-Methoxyphenyl)-1,3-dimethyl-2,3-dihydro-1 <i>H</i> -benzoimidazole. Nano Letters, 2013, 13, 1890-1897.	4.5	129
172	Humidity Effects on Anisotropic Nanofriction Behaviors of Aligned Carbon Nanotube Carpets. ACS Applied Materials & Interfaces, 2013, 5, 9501-9507.	4.0	9
173	Sharp burnout failure observed in high current-carrying double-walled carbon nanotube fibers. Nanotechnology, 2012, 23, 015703.	1.3	11
174	Cu3V2O7(OH)2·2H2O hollow structures for primary lithium batteries. Micro and Nano Letters, 2012, 7, 1101-1104.	0.6	4
175	Anomalous insulator-metal transition in boron nitride-graphene hybrid atomic layers. Physical Review B, 2012, 86, .	1.1	42
176	Synthesis of iron nanoparticles from hemoglobin and myoglobin. Nanotechnology, 2012, 23, 055602.	1.3	23
177	Synthesis of S-doped graphene by liquid precursor. Nanotechnology, 2012, 23, 275605.	1.3	169
178	Deformation and capillary self-repair of carbon nanotube brushes. Carbon, 2012, 50, 5618-5620.	5.4	12
179	Observation of Dynamic Strain Hardening in Polymer Nanocomposites. ACS Nano, 2011, 5, 2715-2722.	7.3	70
180	Conformal Coating of Thin Polymer Electrolyte Layer on Nanostructured Electrode Materials for Three-Dimensional Battery Applications. Nano Letters, 2011, 11, 101-106.	4.5	98

#	Article	IF	CITATIONS
181	Direct Synthesis of Lithium-Intercalated Graphene for Electrochemical Energy Storage Application. ACS Nano, 2011, 5, 4345-4349.	7.3	120
182	Quasi-Molecular Fluorescence from Graphene Oxide. Scientific Reports, 2011, 1, 85.	1.6	253
183	Experimental observation of extremely weak optical scattering from an interlocking carbon nanotube array. Applied Optics, 2011, 50, 1850.	2.1	47
184	Direct laser writing of micro-supercapacitors on hydrated graphite oxide films. Nature Nanotechnology, 2011, 6, 496-500.	15.6	1,322
185	Chemiluminescence determination of cefotaxime sodium with flow-injection analysis of cerium (IV)–rhodamine 6G system and its application to the binding study of cefotaxime sodium to protein with on-line microdialysis sampling. Spectrochimica Acta - Part A: Molecular and Biomolecular Spectroscopy, 2011, 78, 553-557.	2.0	24
186	Thermoplastic Polyurethane Nanocomposites Produced via Impregnation of Long Carbon Nanotube Forests. Macromolecular Materials and Engineering, 2011, 296, 53-58.	1.7	13
187	Effect of Sidewall Fluorination on the Mechanical Properties of Catalytically Grown Multi-Wall Carbon Nanotubes. Materials Research Society Symposia Proceedings, 2011, 1284, 157.	0.1	1
188	Large Scale Growth and Characterization of Atomic Hexagonal Boron Nitride Layers. Nano Letters, 2010, 10, 3209-3215.	4.5	2,317
189	Catalytic performance of Pt nanoparticles on reduced graphene oxide for methanol electro-oxidation. Carbon, 2010, 48, 1124-1130.	5.4	898
190	Atomic layers of hybridized boron nitride and graphene domains. Nature Materials, 2010, 9, 430-435.	13.3	2,002
191	Formation of highly conductive composite coatings and their applications to broadband antennas and mechanical transducers. Journal of Materials Research, 2010, 25, 1741-1747.	1.2	11
192	Modifying Surface Structure to Tune Surface Properties of Vertically Aligned Carbon Nanotube Films. Journal of Nanoscience and Nanotechnology, 2010, 10, 3854-3859.	0.9	2
193	Longitudinal Cutting of Pure and Doped Carbon Nanotubes to Form Graphitic Nanoribbons Using Metal Clusters as Nanoscalpels. Nano Letters, 2010, 10, 366-372.	4.5	323
194	Novel Liquid Precursor-Based Facile Synthesis of Large-Area Continuous, Single, and Few-Layer Graphene Films. Chemistry of Materials, 2010, 22, 3457-3461.	3.2	239
195	Cooperative Adhesion and Friction of Compliant Nanohairs. Nano Letters, 2010, 10, 4509-4513.	4.5	47
196	Design and Reinforcement: Vertically Aligned Carbon Nanotube-Based Sandwich Composites. ACS Nano, 2010, 4, 6798-6804.	7.3	58
197	Effect of Nitrogen Doping on the Mechanical Properties of Carbon Nanotubes. ACS Nano, 2010, 4, 7637-7643.	7.3	65
198	Synthesis and formation mechanism of Cu3V2O7(OH)2·2H2O nanowires. Materials Research Bulletin, 2009, 44, 2027-2032.	2.7	9

#	Article	IF	CITATIONS
199	Graphene Shape Control by Multistage Cutting and Transfer. Advanced Materials, 2009, 21, 4487-4491.	11.1	149
200	Multi-Stable Conductance States in Metallic Double-Walled Carbon Nanotubes. Nanoscale Research Letters, 2009, 4, 538-543.	3.1	1
201	New insights into the structure and reduction of graphite oxide. Nature Chemistry, 2009, 1, 403-408.	6.6	2,355
202	Aligned Carbon Nanotube Stationary Phases for Electrochromatographic Chip Separations. Chromatographia, 2009, 69, 473-480.	0.7	72
203	Engineering Low-Aspect Ratio Carbon Nanostructures: Nanocups, Nanorings, and Nanocontainers. ACS Nano, 2009, 3, 1274-1278.	7.3	51
204	Ionically Self-Assembled Polyelectrolyte-Based Carbon Nanotube Fibers. Chemistry of Materials, 2009, 21, 3062-3071.	3.2	32
205	Transfer Printing of Graphene Using Gold Film. ACS Nano, 2009, 3, 1353-1356.	7.3	115
206	Fabrication and Electrical Characterization of Densified Carbon Nanotube Micropillars for IC Interconnection. IEEE Nanotechnology Magazine, 2009, 8, 196-203.	1.1	30
207	On the synthesis and magnetic properties of multiwall carbon nanotube–superparamagnetic iron oxide nanoparticle nanocomposites. Nanotechnology, 2009, 20, 055607.	1.3	31
208	Synthesis, Characterization, and Electrochemical Properties of Cu <sub>3</sub> V <sub>2</sub> O <sub>7</sub> (OH) <sub>2</sub> ·2H <sub>2</sub> O Nanostructures. Journal of Physical Chemistry C, 2009, 113, 8624-8629.	1.5	59
209	Controlled nanocutting of graphene. Nano Research, 2008, 1, 116-122.	5.8	472
210	On the growth mechanism of nickel and cobalt nanowires and comparison of their magnetic properties. Nano Research, 2008, 1, 465-473.	5.8	47
211	Experimental Observation of an Extremely Dark Material Made By a Low-Density Nanotube Array. Nano Letters, 2008, 8, 446-451.	4.5	614
212	Synthesis of hybrid nanowire arrays and their application as high power supercapacitor electrodes. Chemical Communications, 2008, , 2373.	2.2	180
213	Continuous Carbon Nanotube Reinforced Composites. Nano Letters, 2008, 8, 2762-2766.	4.5	289
214	Nanostructured VO <sub>2</sub> Photocatalysts for Hydrogen Production. ACS Nano, 2008, 2, 1492-1496.	7.3	162
215	Gecko-Inspired Carbon Nanotube-Based Self-Cleaning Adhesives. Nano Letters, 2008, 8, 822-825.	4.5	220
216	Crystalline silicon carbide nanocones and heterostructures induced by released iron nanoparticles. Applied Physics Letters, 2008, 93, 233113.	1.5	16

#	Article	IF	CITATIONS
217	Detecting Mechanical Resonance in Carbon Nanotubes via Inter-Tube Electrical Transport Measurements. Journal of Nanoscience and Nanotechnology, 2008, 8, 436-438.	0.9	0
218	Continuous Carbon Nanotube-PDMS Composites. , 2008, , .		1
219	Air-assisted growth of ultra-long carbon nanotube bundles. Nanotechnology, 2008, 19, 455609.	1.3	66
220	Benchmarking of Metal-to-Carbon Nanotube Side Contact Resistance. , 2008, , .		6
221	Ultralong Aligned Multi-Walled Carbon Nanotube for Electrochemical Sensing. Journal of Nanoscience and Nanotechnology, 2008, 8, 2085-2090.	0.9	9
222	Combined micro-/nanoscale surface roughness for enhanced hydrophobic stability in carbon nanotube arrays. Applied Physics Letters, 2007, 90, 143117.	1.5	87
223	Investigation on Site Density of Carbon Nanotube Forests. Materials Research Society Symposia Proceedings, 2007, 1018, 1.	0.1	0
224	Double-Walled Carbon Nanotube Electrodes for Electrochemical Sensing. Electrochemical and Solid-State Letters, 2007, 10, F13.	2.2	30
225	Flexible energy storage devices based on nanocomposite paper. Proceedings of the National Academy of Sciences of the United States of America, 2007, 104, 13574-13577.	3.3	1,032
226	Polarity-Dependent Electrochemically Controlled Transport of Water through Carbon Nanotube Membranes. Nano Letters, 2007, 7, 697-702.	4.5	176
227	Effects of compressive strains on electrical conductivities of a macroscale carbon nanotube block. Applied Physics Letters, 2007, 91, .	1.5	54
228	Carbon nanotube-based synthetic gecko tapes. Proceedings of the National Academy of Sciences of the United States of America, 2007, 104, 10792-10795.	3.3	400
229	Graphite-like carbon-encapsulated iron nanoparticle self-assembly into macroscopic microtube structures. Journal of Materials Chemistry, 2007, 17, 4619.	6.7	12
230	Vertically Aligned Large-Diameter Double-Walled Carbon Nanotube Arrays Having Ultralow Density. Journal of Physical Chemistry C, 2007, 111, 9077-9080.	1.5	69
231	Vaporâ^'Solid Reaction for Silicon Carbide Hollow Spherical Nanocrystals. Journal of Physical Chemistry C, 2007, 111, 12517-12521.	1.5	50
232	Carbon nanotubes/SiC whiskers composite prepared by CVD method. Diamond and Related Materials, 2007, 16, 531-536.	1.8	16
233	Impact of carbon nanotube exposure, dosage and aggregation on smooth muscle cells. Toxicology Letters, 2007, 169, 51-63.	0.4	91
234	Multifunctional Macroarchitectures of Double-Walled Carbon Nanotube Fibers. Advanced Materials, 2007, 19, 1719-1723.	11.1	52

#	Article	lF	CITATIONS
235	Ultrathick Freestanding Aligned Carbon Nanotube Films. Advanced Materials, 2007, 19, 3300-3303.	11.1	136
236	Densified aligned carbon nanotube films via vapor phase infiltration of carbon. Carbon, 2007, 45, 847-851.	5.4	43
237	Template assembly of tube-in-tube carbon nanotubes grown using Cu as catalyst. Carbon, 2007, 45, 1713-1716.	5.4	9
238	Fatigue resistance of aligned carbon nanotube arrays under cyclic compression. Nature Nanotechnology, 2007, 2, 417-421.	15.6	281
239	Temperature Dependence of the Raman Spectra of Individual Carbon Nanotubes. Journal of Physical Chemistry B, 2006, 110, 1206-1209.	1.2	53
240	Direct growth of aligned carbon nanotubes on bulk metals. Nature Nanotechnology, 2006, 1, 112-116.	15.6	416
241	Effect of H2O adsorption on the electrical transport properties of double-walled carbon nanotubes. Carbon, 2006, 44, 2155-2159.	5.4	51
242	Investigation of the interfacial reaction between multi-walled carbon nanotubes and aluminum. Acta Materialia, 2006, 54, 5367-5375.	3.8	403
243	The reinforcement role of carbon nanotubes in epoxy composites with different matrix stiffness. Composites Science and Technology, 2006, 66, 599-603.	3.8	196
244	Large-Scale Synthesis of Rings of Bundled Single-Walled Carbon Nanotubes by Floating Chemical Vapor Deposition. Advanced Materials, 2006, 18, 1817-1821.	11.1	57
245	Efficiently producing single-walled carbon nanotube rings and investigation of their field emission properties. Nanotechnology, 2006, 17, 2355-2361.	1.3	16
246	Interactions of Carbon Nanomaterials With Mammalian Cells. Materials Research Society Symposia Proceedings, 2006, 951, 8.	0.1	0
247	Multisegmented one-dimensional hybrid structures of carbon nanotubes and metal nanowires. Applied Physics Letters, 2006, 89, 243122.	1.5	39
248	Controllable preparation and properties of single-/double-walled carbon nanotubes. Science and Technology of Advanced Materials, 2005, 6, 725-735.	2.8	13
249	The growth of multi-walled carbon nanotubes with different morphologies on carbon fibers. Carbon, 2005, 43, 663-665.	5.4	118
250	Direct growth of carbon nanotubes on the surface of ceramic fibers. Carbon, 2005, 43, 883-886.	5.4	58
251	Nanoscale carbon tubules deposited in anodic aluminium oxide template: a study of soft x-ray transmission. Chinese Physics B, 2004, 13, 1922-1926.	1.3	3
252	Preparation of double-walled carbon nanotubes. Science Bulletin, 2004, 49, 107-110.	1.7	6

#	Article	IF	CITATIONS
253	Direct Synthesis of a Macroscale Single-Walled Carbon Nanotube Non-Woven Material. Advanced Materials, 2004, 16, 1529-1534.	11.1	131
254	Novel Micro/Nanoscale Hybrid Reinforcement: Multiwalled Carbon Nanotubes on SiC Particles. Advanced Materials, 2004, 16, 2021-2024.	11.1	60
255	Growth of SnO 2 nanowires with uniform branched structures. Solid State Communications, 2004, 130, 89-94.	0.9	148
256	The intrinsic temperature effect of Raman spectra of double-walled carbon nanotubes. Chemical Physics Letters, 2004, 396, 372-376.	1.2	23
257	Random Networks of Single-Walled Carbon Nanotubes. Journal of Physical Chemistry B, 2004, 108, 10751-10753.	1.2	30
258	Hydrogen storage in heat-treated carbon nanofibers prepared by the vertical floating catalyst method. Materials Chemistry and Physics, 2003, 78, 670-675.	2.0	30
259	Double Wall Carbon Nanotubes with an Inner Diameter of 0.4 nm. Chemical Vapor Deposition, 2003, 9, 119-121.	1.4	17
260	Controllable growth of double wall carbon nanotubes in a floating catalytic system. Carbon, 2003, 41, 337-342.	5.4	62
261	Electronic properties of double-walled carbon nanotube films. Carbon, 2003, 41, 2495-2500.	5.4	32
262	Producing cleaner double-walled carbon nanotubes in a floating catalyst system. Carbon, 2003, 41, 2607-2611.	5.4	27
263	Characterization of zinc oxide crystal nanowires grown by thermal evaporation of ZnS powders. Chemical Physics Letters, 2003, 371, 337-341.	1.2	47
264	A simple large-scale synthesis of coaxial nanocables: silicon carbide sheathed with silicon oxide. Chemical Physics Letters, 2003, 375, 269-272.	1.2	22
265	H2-assisted control growth of Si nanowires. Journal of Crystal Growth, 2003, 257, 69-74.	0.7	6
266	Formation of ZnS nanostructures by a simple way of thermal evaporation. Journal of Crystal Growth, 2003, 258, 225-231.	0.7	27
267	Annealing amorphous carbon nanotubes for their application in hydrogen storage. Applied Surface Science, 2003, 205, 39-43.	3.1	70
268	Preparation of highly pure double-walled carbon nanotubes. Journal of Materials Chemistry, 2003, 13, 1340.	6.7	70
269	Raman Characterization and Tunable Growth of Double-Wall Carbon Nanotubes. Journal of Physical Chemistry B, 2003, 107, 8760-8764.	1.2	21
270	Temperature dependence of resonant Raman scattering in double-wall carbon nanotubes. Applied Physics Letters, 2003, 82, 3098-3100.	1.5	69

#	Article	IF	CITATIONS
271	Resonant Raman scattering of double wall carbon nanotubes prepared by chemical vapor deposition method. Journal of Applied Physics, 2003, 94, 5715-5719.	1.1	14
272	Effect of acetylene in buffer gas on the microstructures of carbon nanotubes in arc discharge. Nanotechnology, 2002, 13, L1-L4.	1.3	11
273	Morphologies and microstructures of carbon nanotubes prepared by self-sustained arc discharging. Chinese Physics B, 2002, 11, 496-501.	1.3	6
274	Growth mechanism of Y-junction carbon nanotubes. Diamond and Related Materials, 2002, 11, 1349-1352.	1.8	45
275	Raman scattering and thermogravimetric analysis of iodine-doped multiwall carbon nanotubes. Applied Physics Letters, 2002, 80, 2553-2555.	1.5	43
276	Effect of cupped cathode on microstructures of carbon nanotubes in arc discharge. Carbon, 2002, 40, 1609-1613.	5.4	4
277	Cone-shaped hexagonal 6H–SiC nanorods. Chemical Physics Letters, 2002, 356, 325-330.	1.2	40
278	Preparation of monodispersed multi-walled carbon nanotubes in chemical vapor deposition. Chemical Physics Letters, 2002, 356, 563-566.	1.2	15
279	Double wall carbon nanotubes promoted by sulfur in a floating iron catalyst CVD system. Chemical Physics Letters, 2002, 359, 63-67.	1.2	155
280	Carbon nanofibers and single-walled carbon nanotubes prepared by the floating catalyst method. Carbon, 2001, 39, 329-335.	5.4	133
281	An effective way to lower catalyst content in well-aligned carbon nanotube films. Carbon, 2001, 39, 152-155.	5.4	55
282	Hydrogen uptake by graphitized multi-walled carbon nanotubes under moderate pressure and at room temperature. Carbon, 2001, 39, 2077-2079.	5.4	86
283	Vertical aligned carbon nanotubes grown on Au film and reduction of threshold field in field emission. Chemical Physics Letters, 2001, 335, 150-154.	1.2	55
284	Controllable growth of single wall carbon nanotubes by pyrolizing acetylene on the floating iron catalysts. Chemical Physics Letters, 2001, 349, 191-195.	1.2	72
285	Crystallization behavior of the amorphous carbon nanotubes prepared by the CVD method. Journal of Crystal Growth, 2001, 233, 823-828.	0.7	104
286	Preparation of carbon nanofibers by the floating catalyst method. Carbon, 2000, 38, 1933-1937.	5.4	96
287	Novel carbon filaments with carbon beads grown on their surface. Journal of Materials Science Letters, 2000, 19, 21-22.	0.5	2
288	Title is missing!. Journal of Materials Science Letters, 2000, 19, 1769-1770.	0.5	0

#	Article	IF	CITATIONS
289	Deposition of the platinum crystals on the carbon nanotubes. Science Bulletin, 2000, 45, 134-137.	1.7	12
290	Graphitization behavior of carbon nanofibers prepared by the floating catalyst method. Materials Letters, 2000, 43, 291-294.	1.3	28
291	Phosphorus - a new element for promoting growth of carbon filaments by the floating catalyst method. Carbon, 1999, 37, 1652-1654.	5.4	12
292	Preparation of Carbon Nanotubules by the Floating Catalyst Method. Journal of Materials Science Letters, 1999, 18, 797-799.	0.5	19